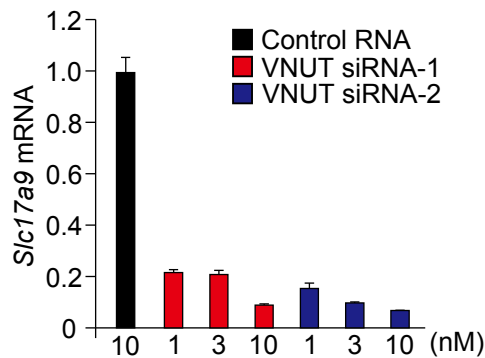


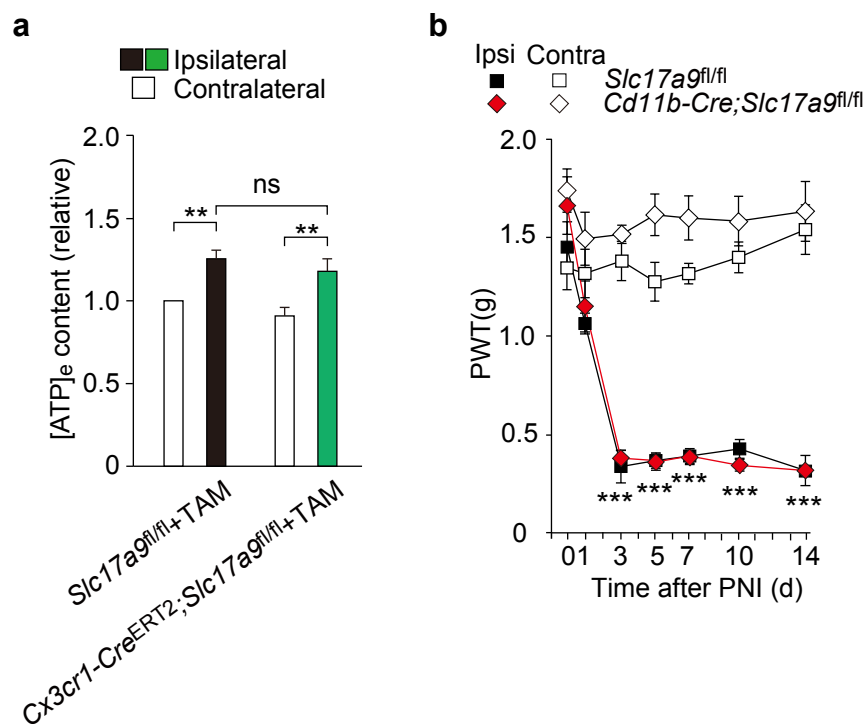
Supplementary Figure 1. PNI increases an extracellular ATP level within the spinal cord 3 days, but not 28 days, after PNI.

Measurement of [ATP]_e content in the ACSF media of ipsilateral and contralateral spinal cord slices taken from wild-type mice (a) 3 days and (b) 28 days after PNI. Values represent the relative ratio of ATP levels to the contralateral side (a, $n=13$; b, $n=8$; *** $P=0.0007$ vs. Contralateral, Wilcoxon matched-pairs signed rank test). Values are means \pm s.e.m.



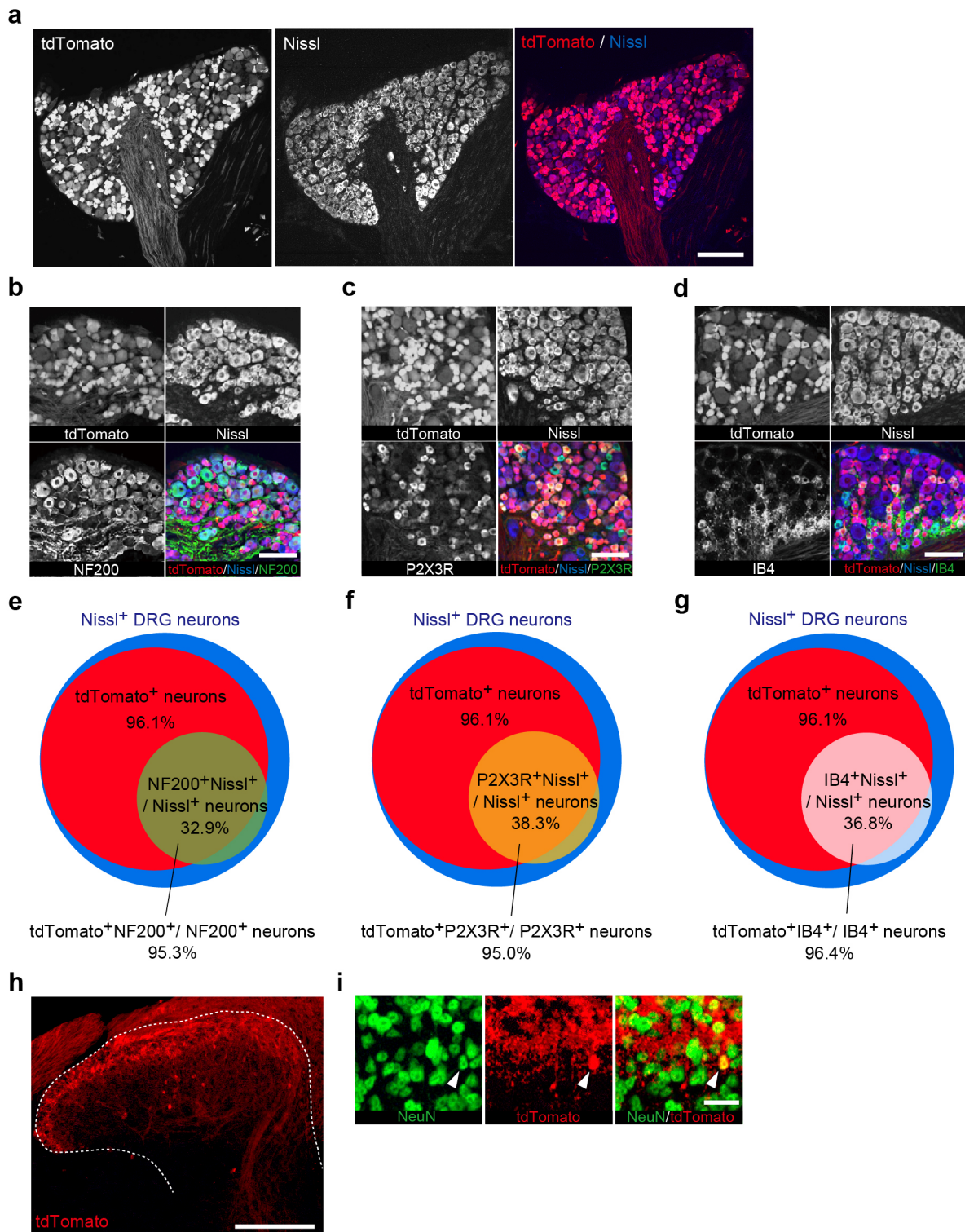
Supplementary Figure 2. Effect of siRNAs on VNUT expression.

Real-time PCR analysis of *Slc17a9* mRNA in BV2 cells treated with control RNA (10 nM) or VNUT siRNAs (1, 3, 10 nM) for 48 h. Values represent the relative ratio of *Slc17a9* mRNA (normalized to the value for 18s mRNA) to the control RNA ($n=3$). Values are means \pm s.e.m.



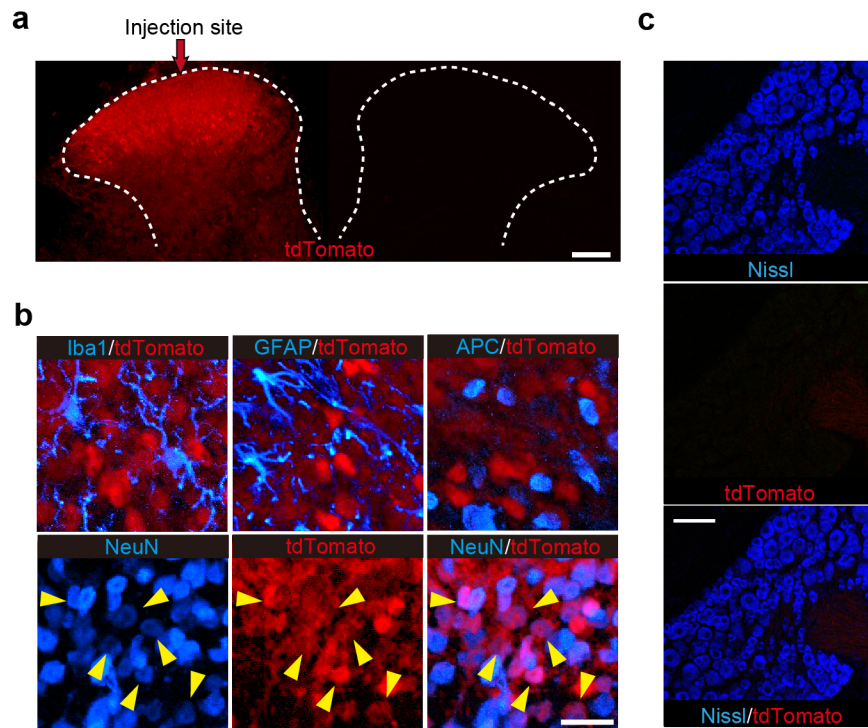
Supplementary Figure 3. Microglial VNUT is not required for PNI-induced increase in extracellular ATP within the spinal cord and pain hypersensitivity.

(a) Measurement of [ATP]_e content in the ACSF media of spinal cord slices isolated from *Slc17a9^{fl/fl}* or *Cx3cr1-Cre^{ERT2};Slc17a9^{fl/fl}* mice that had been injected with tamoxifen (TAM), 7 days after PNI ($n=14$; $**P<0.01$, one-way ANOVA with post hoc Tukey Multiple Comparison test). (b) PWT of microglia-specific VNUT conditional knockout (*Cd11b-Cre;Slc17a9^{fl/fl}*) mice and their *Slc17a9^{fl/fl}* littermate controls before and after PNI [*Slc17a9^{fl/fl}*: $n=5$, *Cd11b-Cre;Slc17a9^{fl/fl}*: $n=6$; $***P<0.001$ vs. Contra (*Slc17a9^{fl/fl}*), two-way ANOVA with post hoc Bonferroni test]. Values are means \pm s.e.m.



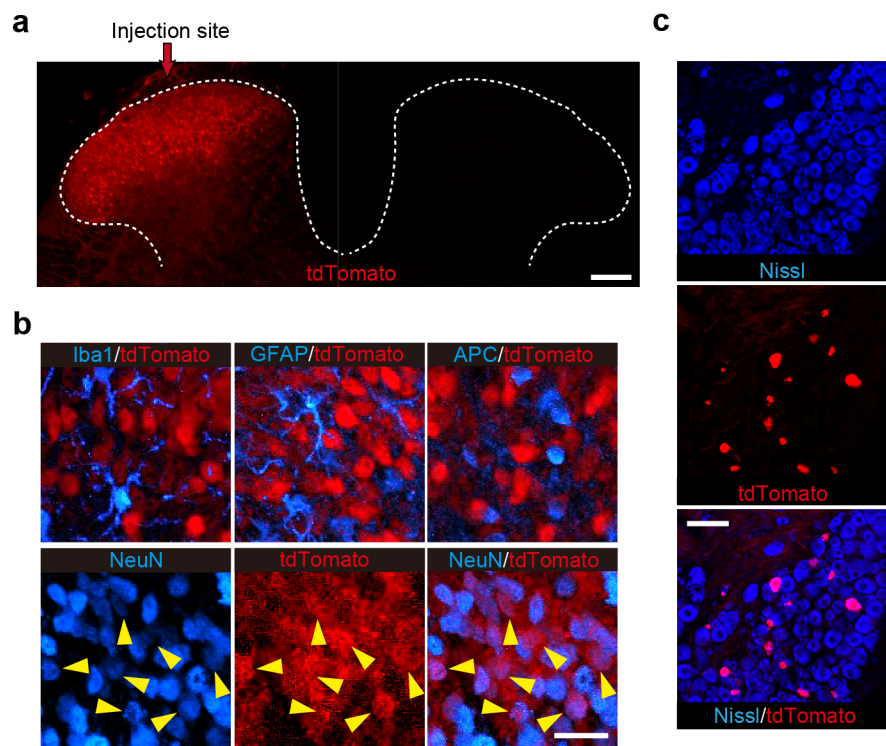
Supplementary Figure 4. AAV-mediated Cre recombination in DRG neurons.

(a) Representative images (of three experiments) showing tdTomato fluorescence and Nissl staining in the L4 DRG of ROSA26 (R26)-tdTomato reporter mice intraperitoneally injected with AAV-ESYN-Cre vector. (scale bar, 200 μ m) **(b-d)** Representative images (of three experiments) showing fluorescent signals of tdTomato with Nissl staining and immunofluorescence labelling of **(b)** NF200, **(c)** P2X3R or **(d)** IB4 in the L4 DRG of R26-tdTomato mice treated with AAV-ESYN-Cre vector. (scale bar, 100 μ m) **(e-g)** Charts summarize the results of Supplementary Figures 3b-d showing the distribution of tdTomato-positive DRG neurons. **(h)** Representative images (of three experiments) showing tdTomato fluorescence in the L4 spinal cord of R26-tdTomato mice intraperitoneally injected with AAV-ESYN-Cre vector. (scale bar, 200 μ m) **(i)** Fluorescent signals of tdTomato and immunofluorescence labelling of NeuN in the L4 spinal cord of R26-tdTomato mice treated with AAV-ESYN-Cre vector. Arrowhead indicates colocalization of tdTomato signal with NeuN signal. (scale bar, 20 μ m)



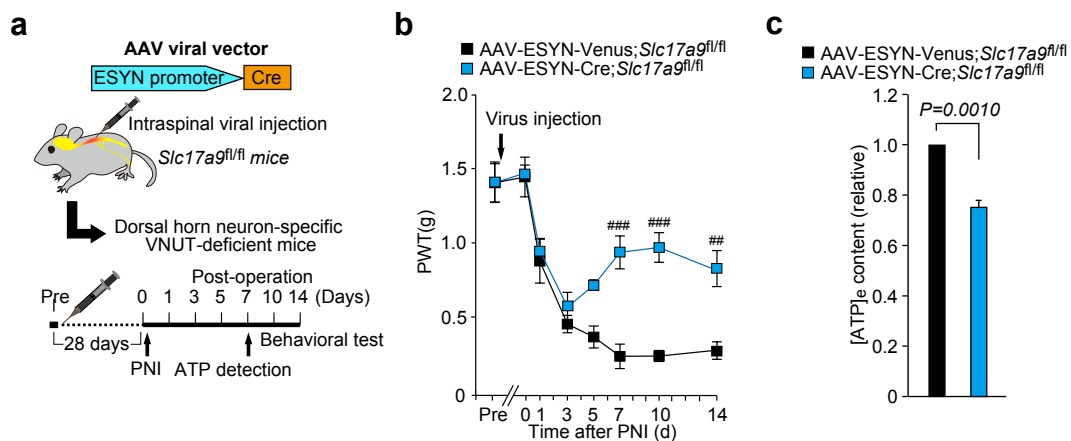
Supplementary Figure 5. AAV-mediated Cre recombination in spinal dorsal horn neurons.

(a) Representative images (of three experiments) showing tdTomato fluorescence in the L4 spinal cord of R26-tdTomato mice intraspinally injected with AAV-NSE-Cre vector. (scale bar, 100 μ m) **(b)** Representative images (of three experiments) showing tdTomato fluorescence with immunofluorescent labelling of Iba1 (microglia), GFAP (astrocyte), APC (oligodendrocyte) or NeuN (neuron) in the L4 spinal cord of R26-tdTomato mice treated with AAV-NSE-Cre vector. Arrowheads indicate colocalization of tdTomato signals with NeuN signals. (scale bar, 20 μ m) **(c)** Representative images (of three experiments) showing Nissl staining with tdTomato fluorescence in the L4 DRG of R26-tdTomato mice treated with AAV-NSE-Cre vector. (scale bar, 100 μ m)



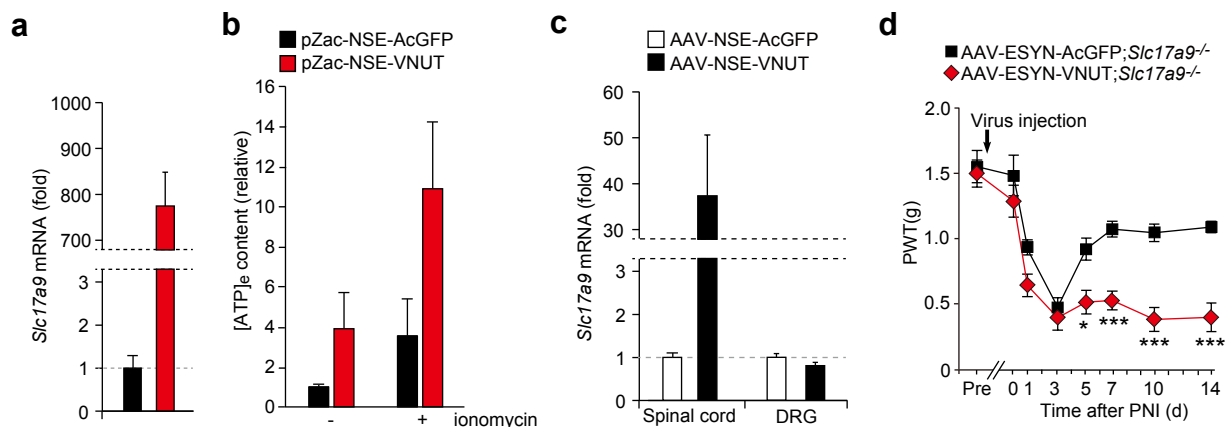
Supplementary Figure 6. AAV-mediated Cre recombination in spinal dorsal horn neurons.

(a) Representative images (of three experiments) showing tdTomato fluorescence in the L4 spinal cord of R26-tdTomato mice intraspinally injected with AAV-ESYN-Cre vector. (scale bar, 100 μ m) **(b)** Representative images (of three experiments) showing tdTomato fluorescence with immunofluorescent labelling of Iba1 (microglia), GFAP (astrocyte), APC (oligodendrocyte) or NeuN (neuron) in the L4 spinal cord of R26-tdTomato reporter mice treated with AAV-ESYN-Cre vector. Arrowheads indicate colocalization of tdTomato signals with NeuN signals. (scale bar, 20 μ m) **(c)** Representative images (of three experiments) showing Nissl staining with tdTomato fluorescence in the L4 DRG of R26-tdTomato mice treated with AAV-ESYN-Cre vector. A small number of Nissl-positive DRG neurons was positive to tdTomato (8.47%: 103 of 1216 Nissl⁺ cells). (scale bar, 100 μ m)



Supplementary Figure 7. VNUT expressed in SDH neurons is involved in increased spinal ATP supply and pain hypersensitivity after PNI.

(a) Schematic diagram of the experimental protocol. **(b)** PWT of *Slc17a9^{fl/fl}* mice intraspinally injected with AAV-ESYN-Venus or an AAV-ESYN-Cre viral vectors before and after PNI (AAV-ESYN-Venus;*Slc17a9^{fl/fl}*: $n=5$, AAV-ESYN-Cre;*Slc17a9^{fl/fl}*: $n=6$; ## $P<0.01$, ### $P<0.001$ vs. AAV-ESYN-Venus;*Slc17a9^{fl/fl}*, two-way ANOVA with post hoc Bonferroni test) **(c)** Measurement of [ATP]_e content in the ACSF media of spinal cord slices isolated from *Slc17a9^{fl/fl}* mice intraspinally injected with AAV-ESYN-Venus or AAV-ESYN-Cre vectors 7 days after PNI ($n=11$, Wilcoxon matched-pairs signed rank test).



Supplementary Figure 8. Ectopic expression of VNUT in dorsal horn neurons of *Slc17a9*^{-/-} mice rescues tactile allodynia after PNI.

(a) Real-time PCR analysis of *Slc17a9* mRNA using total RNA extracted from neuronal cell line Neuro2A cells, transduced with pZac-NSE-AcGFP or pZac-NSE-VNUT vectors. Values represent the relative ratio of *Slc17a9* mRNA (normalized to the value for *18s* mRNA) to cells with pZac-NSE-AcGFP ($n=6$). **(b)** Measurement of [ATP]_e content in the culture media of Neuro2A cells, transduced with pZac-NSE-AcGFP or pZac-NSE-VNUT, with or without treatment of Ca²⁺ ionophore ionomycin (5 μ M) for 20 min. Values represent the relative ratio of ATP levels to the control ($n=5$). **(c)** Real-time PCR analysis of *Slc17a9* mRNA using total RNA extracted from the spinal cord and the DRG of WT mice 28 days after intraspinal viral vector injection (AAV-NSE-AcGFP or AAV-NSE-VNUT). Values represent the relative ratio of *Slc17a9* mRNA (normalized to the value for *18s* mRNA) to the AAV-NSE-AcGFP mice ($n=6$). **(d)** PWT of *Slc17a9*^{-/-} mice intraspinally injected with AAV-ESYN-AcGFP or AAV-ESYN-VNUT viral vectors before and after PNI (AAV-ESYN-AcGFP; *Slc17a9*^{-/-}: $n=6$, AAV-ESYN-VNUT; *Slc17a9*^{-/-}: $n=7$, * $P<0.05$, *** $P<0.001$ vs. AAV-ESYN-AcGFP; *Slc17a9*^{-/-}, two-way ANOVA with post hoc Bonferroni test). Values are means \pm s.e.m.